

Supplementary Materials

Removal of the Water Pollutant Ciprofloxacin Using Biodegradable Sorbent Polymers Obtained from Polysaccharides

**Sarah Alvarado^{1,†}, Alicia Megia-Fernandez^{1,2,3}, Mariano Ortega-Muñoz^{1,2,3},
Fernando Hernandez-Mateo^{1,2,3}, F. Javier Lopez-Jaramillo^{1,2,3,*} and Francisco Santoyo-Gonzalez^{1,2,3,*}**

¹ Department Organic Chemistry, Faculty of Sciences, University of Granada, 18073 Granada, Spain

² Unit of Excellence in Chemistry Applied to Biomedicine and the Environment, University of Granada, 18073 Granada, Spain

³ Biotechnology Institute, University of Granada, 18071 Granada, Spain

* Correspondence: fjljara@ugr.es (F.J.L.-J.); fsantoyo@ugr.es (F.S.-G.)

† Current address: Institute for Advanced Chemistry of Catalonia, CSIC, 08034 Barcelona, Spain.

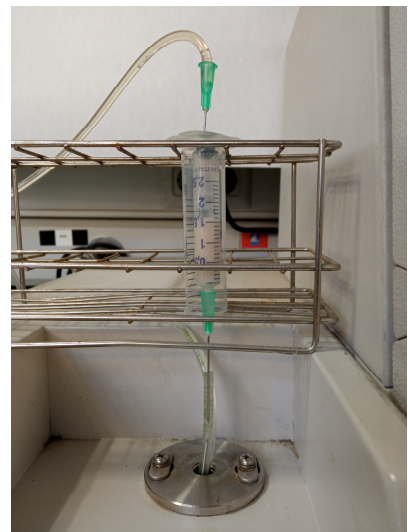


Figure. S1. (a) General setting for the fixed bed studies with pSt. (b) Detail of the pSt packing.

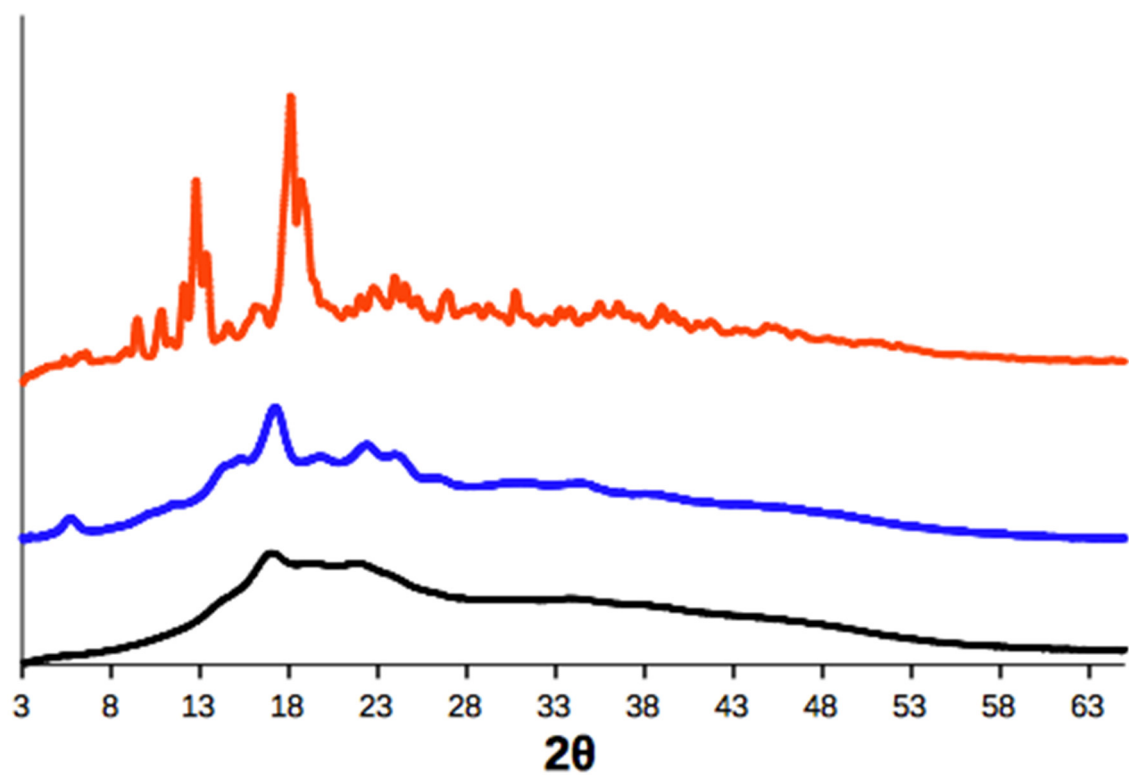


Figure. S2. DRX of the starting material β -CD (red) St (blue) and Dx (black) showing the d-spacing of some peaks.

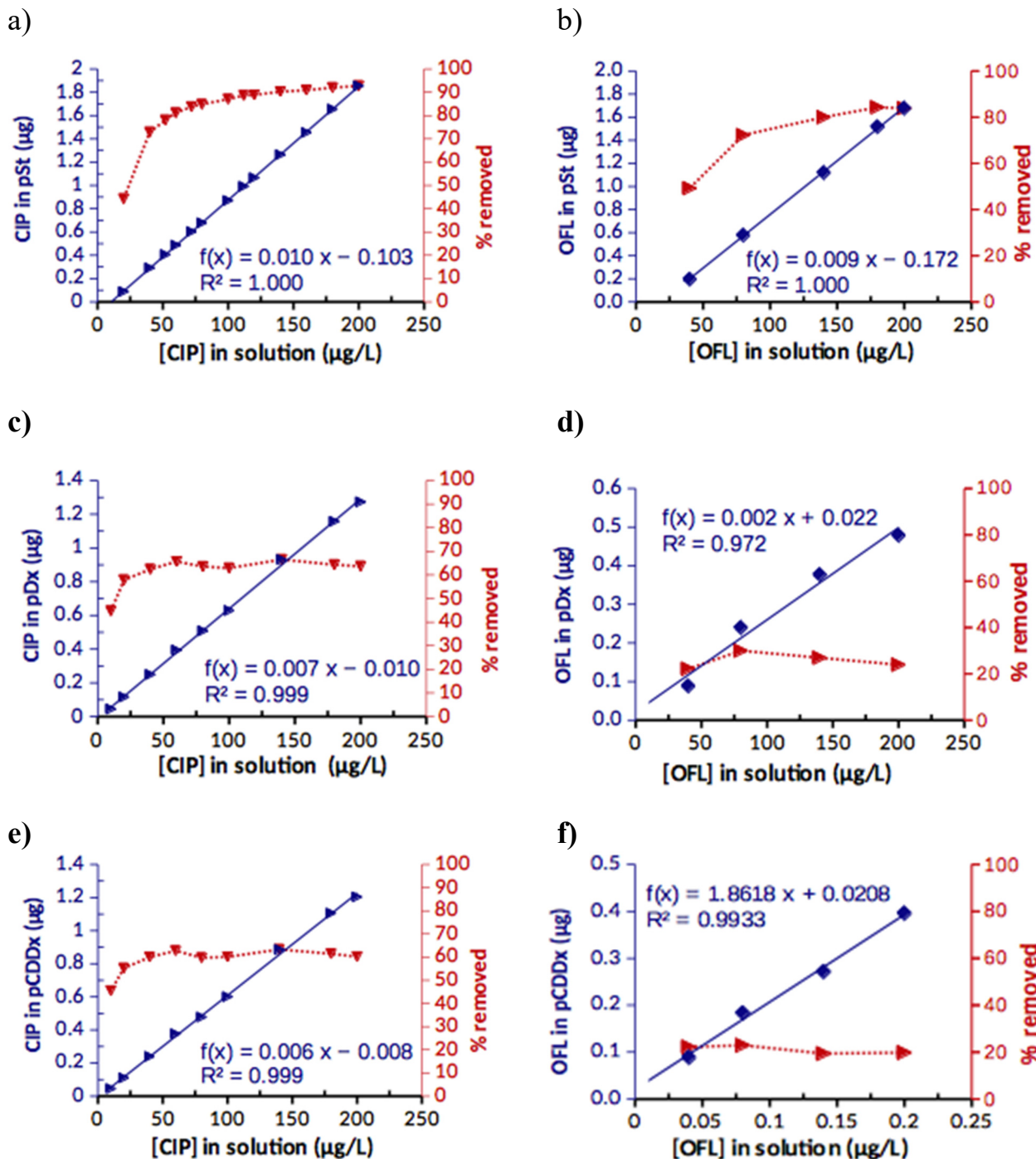


Figure. S3. Characterization of the polymers pSt (a & b), pDx (c & d) and pCD-Dx (e & f) as sorbent for CIP (a, c, e) and OFL (b, d, f). In blue, amount retained by the polymer and in red the percentage removed from the solution as a function of the initial concentration of quinolone.

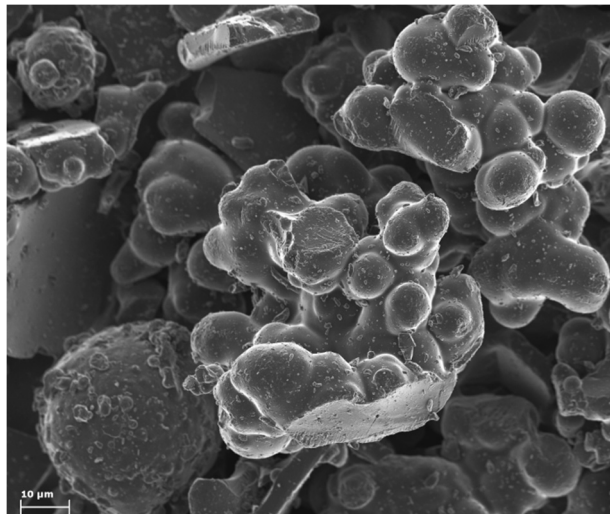


Figure. S4. SEM micrograph of pCD-Dx at 10.00 K x.

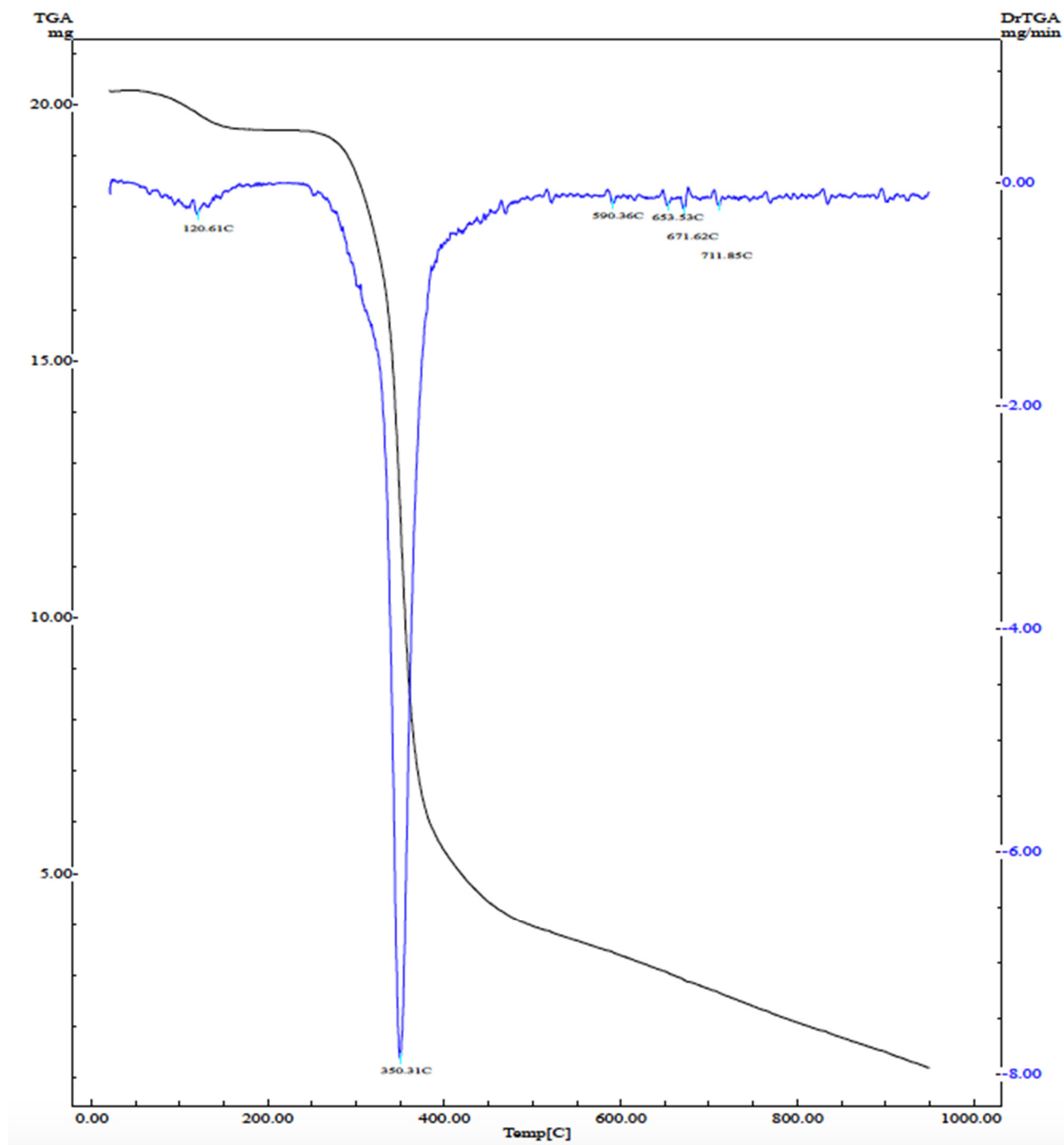


Figure. S5 Derivative TGA of pSt. In black is shown the evolution of the mass of the sample as a function of the temperature and in blue the first derivative

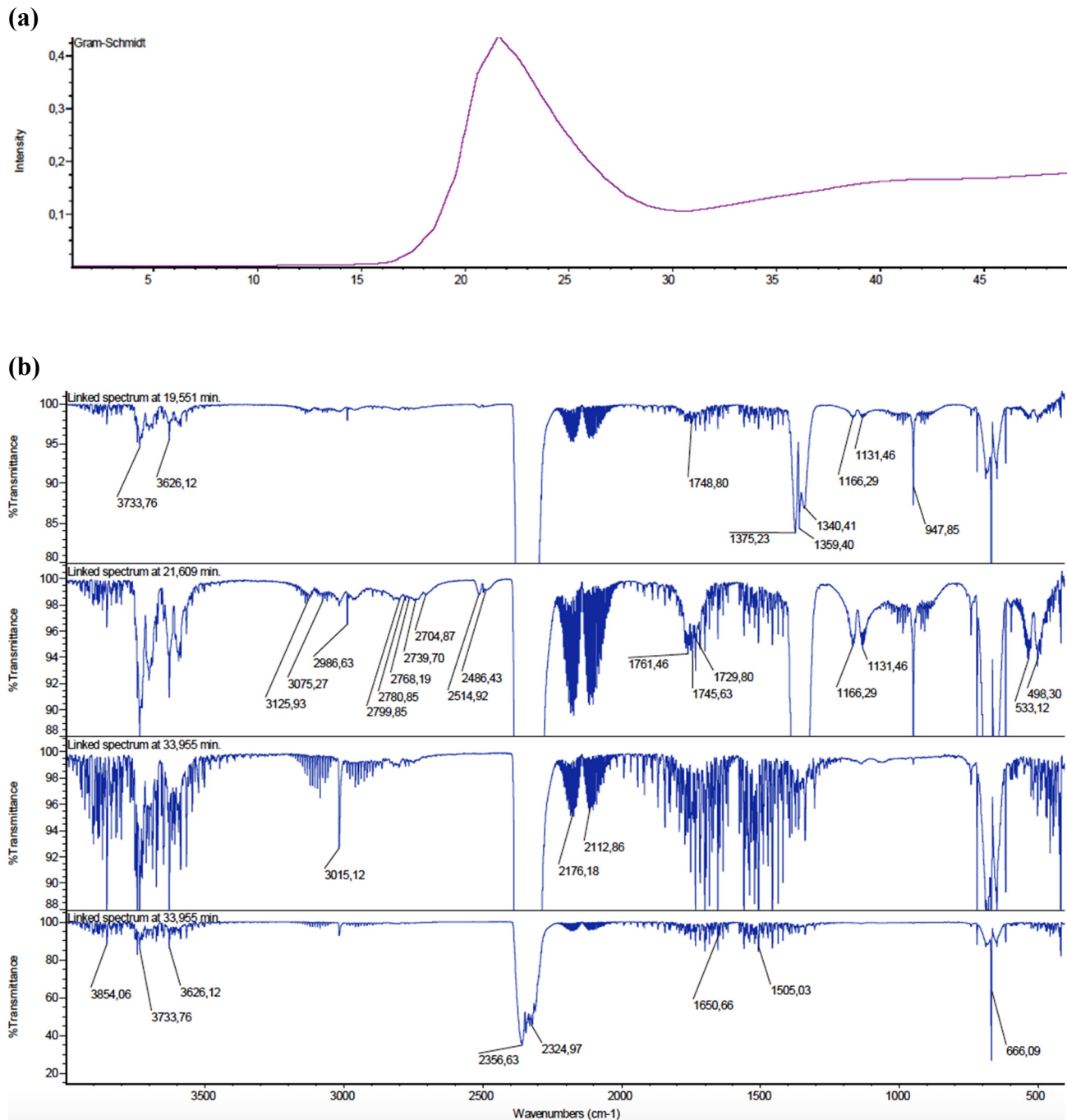
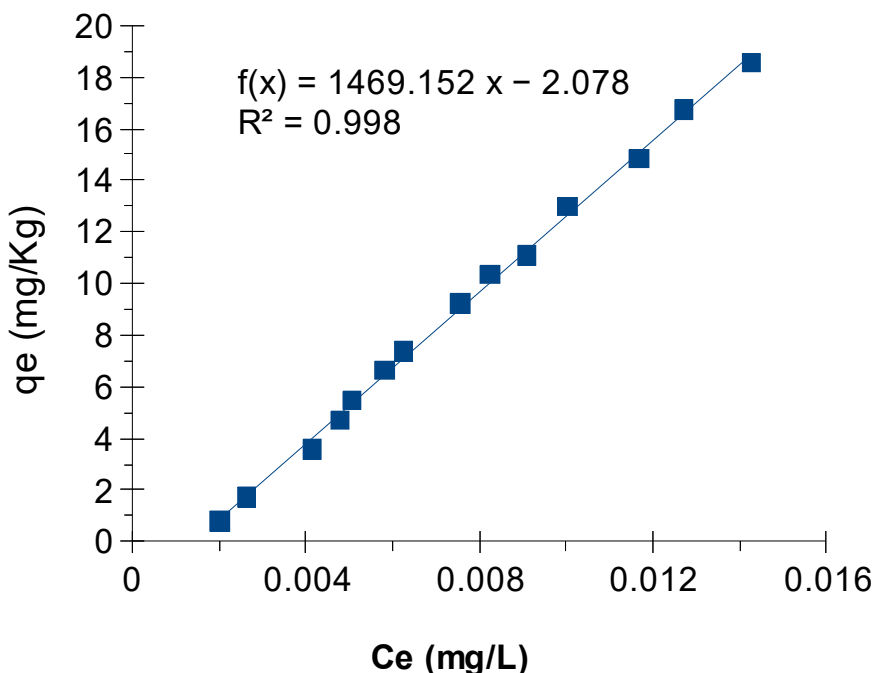


Figure. S6. IR-TGA of pSt. (a) Gram-Schmidt. (b) Most representative signals at three single time points 19.6 min, 21.6 min and 34.0 min. The delay between the TG and the FTIR detector is from 4 to 5 min.

(a)



(b)

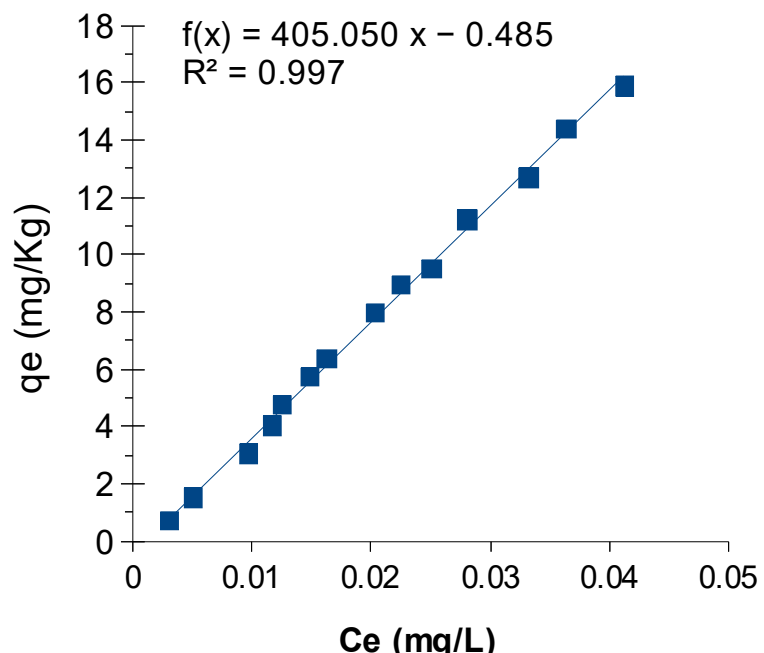


Figure. S7. Estimation of the sorption coefficient of CIP (a) and OFL (b) on pSt.

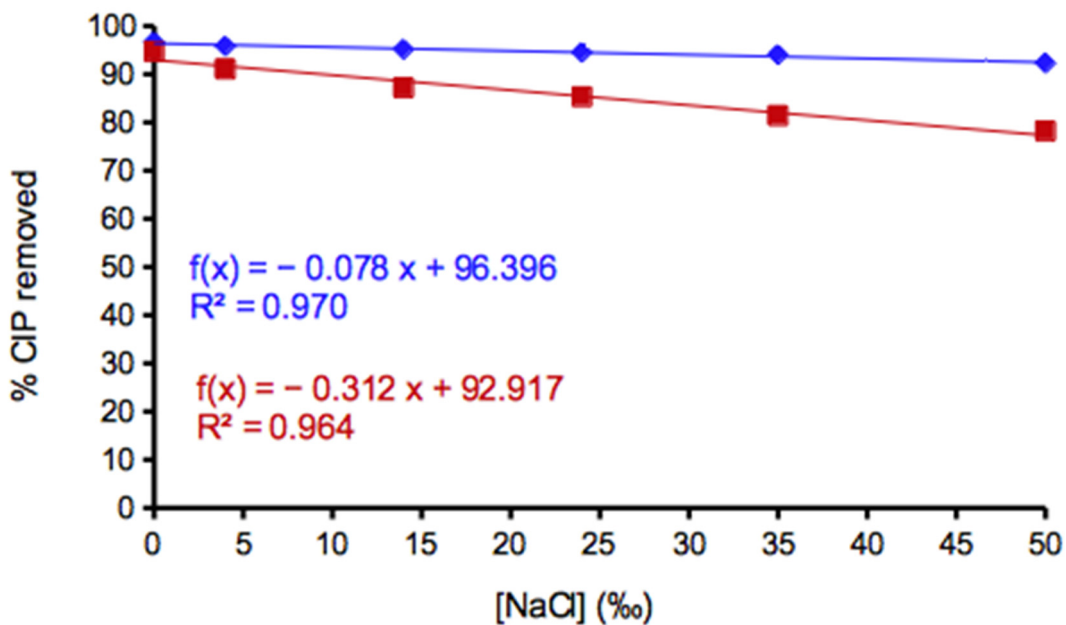
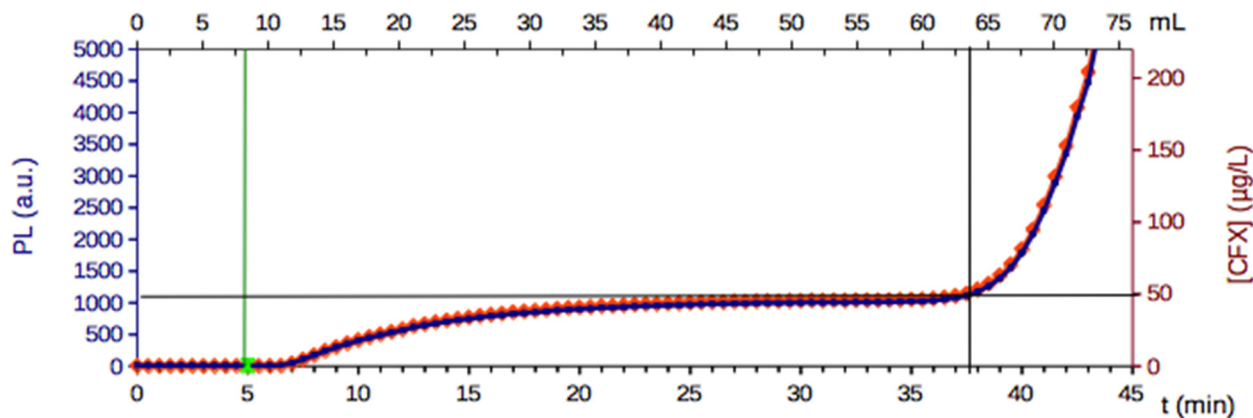


Figure. S8. Negative effect of the salinity on the sorption of CIP on pSt (red) and improvement of the performance by buffering to pH 8 (blue)

(a)



(b)

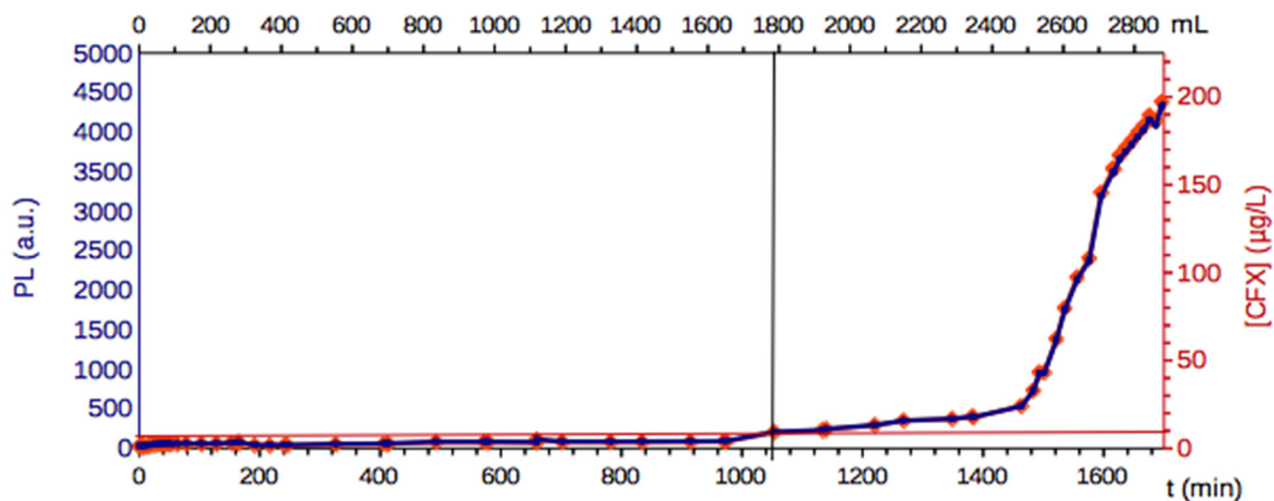


Figure. S9. Fixed bed studies of the sorption of CIP on pSt. Photoluminescence (arbitrary units, in blue) and concentration of CIP ($\mu\text{g}/\text{L}$, in red) of a solution of 10 mg/L (a) and 200 $\mu\text{g}/\text{L}$ (b) flown through the regenerated pSt (0.5 g) packed into a 2.5 mL syringe. The green line in (a) marks the initiation of pumping the solution of CIP.

Table S1. Equations of the isotherm model assayed for the fitting of the experimental sorption data as defined by ISOT_calc [31,43].

Isotherm (# parameters)	Equation ($q_e = \dots$)	Parameter definition [43]
Langmuir (2)	$S_T \frac{K_L \cdot C_e}{1 + K_L \cdot C_e}$	S_T is maximum adsorption capacity K_L is affinity constant
Freundlich (2)	$K_F \cdot C_e^N$	K_F is adsorption potential N is strength constant associated to heterogeneity (for homogenous systems $N=1$)
Temkin (2)	$k_1 \cdot \ln(C_e) + k_2$	k_1 and k_2 are constants of Temkin isotherm and k_1 is related to sorption heat
Vieth-Sladek (3)	$K_D \cdot C_e + \frac{S_T \cdot b \cdot C_e}{1 + b \cdot C_e}$	K_D and b are Vieth-Sladek constants S_T is the maximum adsorption capacity
Redlich-Peterson (3)	$S_T \frac{k \cdot C_e}{1 + (k \cdot C_e)^N}$	S_T is maximum adsorption capacity k is related to constants of Redlich-Peterson model N ranges from 0 to 1
2-sites Langmuir (4)	$\frac{S_{T1} \cdot k_1 \cdot C_e}{1 + k_1 \cdot C_e} + \frac{S_{T2} \cdot k_2 \cdot C_e}{1 + k_2 \cdot C_e}$	S_{T1} and S_{T2} are the maximum adsorption capacity for sites 1 and 2 K_1 and K_2 are affinity constant for sites 1 and 2

Table S2. Elemental analysis of cross-linked polymers. Results are expressed as means ± SD(n = 3)

	pSt	pDx	pCD-Dx
% C	41.04 ± 1.387	39.77 ± 0.381	40.13 ± 0.255
% H	7.45 ± 0.236	7.49 ± 0.307	7.81 ± 0.116
% S	7.16 ± 0.453	7.40 ± 0.080	7.51 ± 0.163

Table S3. Isotherm models that fail the non-linear fitting of the sorption of CIP and OFL on pSt.

	Langmuir	Vieth-Sladek	Redlich-Peterson	2 sites Langmuir
CIP-pSt	$S_T=1.033 \times 10^3$ <i>r.s.d. (%)=1.6x10³</i> $K_L=1.119 \times 10^0$ <i>r.s.d. (%)=1.6x10³</i> $MWSE=4.82 \times 10^{-2}$	$K_D=1.144 \times 10^3$ <i>r.s.d. (%)=7.7x10⁰</i> $S_T=1.000 \times 10^{-1}$ <i>r.s.d. (%)=2.6x10⁶</i> $b=1.000 \times 10^0$ <i>r.s.d. (%)=2.6x10⁶</i> $MWSE=4.71 \times 10^{-2}$	$S_T=2.619 \times 10^3$ <i>r.s.d. (%)=1.8x10⁶</i> $K=8.733 \times 10^{-1}$ <i>r.s.d. (%)=1.8x10⁶</i> $N=1.000 \times 10^0$ <i>r.s.d. (%)=2.6x10⁶</i> $MWSE=4.71 \times 10^{-2}$	$S_{T1}=1.038 \times 10^3$ <i>r.s.d. (%)=1.8x10³</i> $K_{L1}=1.114 \times 10^0$ <i>r.s.d. (%)=1.8X10³</i> $S_{T2}=1.020 \times 10^3$ <i>r.s.d. (%)=2.7x10⁶</i> $K_{L2}=1.114 \times 10^{-3}$ <i>r.s.d. (%)=2.7x10⁶</i> $MWSE=4.82 \times 10^{-2}$
OFL-pSt	$S_T=5.468 \times 10^5$ <i>r.s.d. (%)=1.2x10⁵</i> $K_L=6.381 \times 10^{-4}$ <i>r.s.d. (%)=1.2x10⁵</i> $MWSE=1.29 \times 10^{-2}$	$K_D=3.666 \times 10^2$ <i>r.s.d. (%)=4.3x10⁰</i> $S_T=1.000 \times 10^0$ <i>r.s.d. (%)=1.3x10⁶</i> $b=1.000 \times 10^0$ <i>r.s.d. (%)=1.3x10⁶</i> $MWSE=1.14 \times 10^{-2}$	$S_T=1.023 \times 10^3$ <i>r.s.d. (%)=8.9x10⁵</i> $K=7.164 \times 10^{-1}$ <i>r.s.d. (%)=8.9x10⁵</i> $N=1.000 \times 10^0$ <i>r.s.d. (%)=1.3x10⁶</i> $MWSE=1.14 \times 10^{-2}$	$S_{T1}=5.605 \times 10^5$ <i>r.s.d. (%)=5.1x10⁵</i> $K_{L1}=6.540 \times 10^{-4}$ <i>r.s.d. (%)=5.1X10⁵</i> $S_{T2}=5.468 \times 10^3$ <i>r.s.d. (%)=1.3x10⁶</i> $K_{L2}=6.381 \times 10^{-4}$ <i>r.s.d. (%)=1.3x10⁶</i> $MWSE=1.14 \times 10^{-2}$

References

31. Beltrán, J.L.; Pignatello, J.J.; Teixidó, M. ISOT_Calc: A Versatile Tool for Parameter Estimation in Sorption Isotherms. *Comput. Geosci.* **2016**, *94*, 11–17. <https://doi.org/10.1016/j.cageo.2016.04.008>.
43. Majd, M.M.; Kordzadeh-Kermani, V.; Ghalandari, V.; Askari, A.; Sillanpää, M. Adsorption Isotherm Models: A Comprehensive and Systematic Review (2010–2020). *Sci. Total Environ.* **2022**, *812*, 151334. <https://doi.org/10.1016/j.scitotenv.2021.151334>.